Conception, realization and characterization of a very high negative chromatic dispersion fiber

Jean-Louis Auguste, Jean-Marc Blondy, Julien Maury, Jacques Marcou, Bernard Dussardier, Gérard Monnom, Rajeev Jindal, Krishna Thyagarajan, Bishnu P. Pal

▶ **To cite this version:**

Jean-Louis Auguste, Jean-Marc Blondy, Julien Maury, Jacques Marcou, Bernard Dussardier, et al.. Conception, realization and characterization of a very high negative chromatic dispersion fiber. Optical Fiber Technology, 2002, 8, pp.89-105. hal-00469705

HAL Id: hal-00469705
https://hal.science/hal-00469705

Submitted on 6 Apr 2010

HAL is a multi-disciplinary open access archive for the deposit and dissemination of scientific research documents, whether they are published or not. The documents may come from teaching and research institutions in France or abroad, or from public or private research centers.

L'archive ouverte pluridisciplinaire **HAL**, est destinée au dépôt et à la diffusion de documents scientifiques de niveau recherche, publiés ou non, émanant des établissements d'enseignement et de recherche français ou étrangers, des laboratoires publics ou privés.

Invited Paper

Conception, Realization, and Characterization of a Very High Negative Chromatic Dispersion Fiber

J. L. Auguste,* J. M. Blondy,* J. Maury,* J. Marcou,*
B. Dussardier,† G. Monnom,† R. Jindal,†
K. Thyagarajan,‡ and B. P. Pal‡

*E.O.G.I., I.R.C.O.M. (UMR 6615), 123, av. A. Thomas, 87060 Limoges Cedex, France;
†L.P.M.C. Groupe Guides Optiques Actifs (UMR 6622), Parc Valrose, 06108 Nice Cedex, France; and
‡Physics Dept., Indian Institute of Technology, Hauz Khas, New Delhi 110016, India
E-mail: auguste@ircom.unilim.fr, monnom@unice.fr, bppal@physics.iitd.ernet.in

Received August 1, 2001; revised October 8, 2001

After a brief presentation of many possible solutions usable to control or compensate the chromatic dispersion of optical links, we report the simulation, realization, and characterization of a dual asymmetric core dispersion compensating optical fiber. The simulation stage, using a cylindrical coordinates B.P.M., determines the optimized refractive index profile of the dispersion compensating fiber (DCF) including the optogeometrical tolerances, like the effect of the central index dip obtained by MCVD process. The realized fiber is characterized by phase shift method to measure its chromatic dispersion. The dispersion coefficient was measured to be −1800 ps/(nm·km) in the 1.55-μm low-loss window. A study of the propagation behavior and measurements of connection, propagation, and bending losses of this fiber are also presented. © 2002 Elsevier Science (USA)

1. INTRODUCTION

The Internet revolution and the consequent enormous growth in demand for transmission capacity have led to intense research activities on dense wavelength division multiplexed optical transmission (DWDM). In recent years DWDM optical

communication is seeing a steady migration from 2.5 to 10 Gb/s over each wavelength spanning the entire erbium-doped fiber amplifiers (EDFA) gain bandwidth and thus achieve higher *spectral efficiency*, which is defined as the *ratio* of average transmission rate to channel spacing. With the wide availability of EDFAs and imminent arrival of 40 Gb/s systems, temporal dispersion compensation/management has assumed great importance as it is the main impairing factor for achieving repeaterless transmission distance in excess of 100 km over standard single-mode fibers [1].

One of the earliest techniques suggested to reduce the dispersion at the 1.55-μm band was to tailor the refractive index profile of a single-mode fiber in such a way that its zero dispersion wavelength is shifted from the conventional 1.31-μm window to around 1.55-μm [2]. These fibers, called dispersion-shifted fibers (DSF), though appeared promising for a while were, however, were found to be unusable in a DWDM link due to the fact that operating a fiber with near zero-dispersion is known to introduce nonlinear effects like four-wave mixing (FWM) [3]. It is known that FWM effect can be greatly reduced by allowing a small but finite local dispersion all along a DWDM link. This task could be fulfilled either through dispersion management, i.e., by combining alternate lengths of positive and negative dispersion fibers [4] or by employing so-called nonzero dispersion-shifted fibers (NZ-DSF) [5, 6]. As per ITU recommendation, NZ-DSF fibers, generically referred to as G.655 fibers, were designed to leave a small residual average dispersion of 2–6 ps/(nm·km) to counter nonlinear propagation effects in a single-mode fiber.

On the other hand, millions of kilometers of installed optical links around the world operate with 1.31-μm optimized G.652 type of single-mode fibers. Due to the availability of EDFAs and also because of lower loss at the 1.55-μm band, there has been a substantial interest to operate these installed fibers at the 1.55-μm band. Unfortunately, when operated at the 1.55-μm band these fibers exhibit chromatic dispersion of 16–18 ps/(nm·km). Thus in order to achieve repeaterless link lengths in excess of 100 km, which is the typical desirable spacing between EDFAs in a long-haul optical link, one requires insertion of some dispersion compensating device(s)/component(s) to mitigate the cumulated chromatic dispersion in an actual link.

Chromatic dispersion is a linear effect and inserting a component with opposite sign could greatly reduce its detrimental effect in G.652 fibers at the 1.55-μm band. Out of the several different techniques that have been proposed in the literature, the ones which seem to hold immediate promise could be classified as dispersion compensating fibers (DCF) [7], chirped fiber Bragg gratings (FBG) [8, 9], high-order mode (HOM) fibers [10], virtual-imaged phased-array-based microoptic device [11]. In a chirped grating the optical pitch (product between the grating period and the mode effective index) varies along length of the FBG. As a result resonant reflection frequency of the FBG becomes a function of position along length of the FBG. Thus each frequency component of a propagating pulse is reflected from a different point along length of the chirped FBG. Thus depending on sign of the chirp, a chirped FBG could impart either a positive or negative dispersion to a propagating pulse [12]. Since dispersion compensation is achieved on reflection, to access the dispersion corrected pulse, an optical circulator or a fiber coupler is required as an additional component with associated insertion loss.

Furthermore, errors in the chirped phase mask periodicity could lead to ripples in group delay with wavelength. In a recent proposal use of a long-period FBG has been suggested to compensate dispersion in transmission [13]. The HOM technique exploits large negative dispersion and dispersion slope, which are characteristics of higher order modes of a fiber relative to the fundamental mode. Thus one requires a fiber, which supports more than one mode at the operating wavelengths. Further, conversion of power from fundamental to a higher order mode and reconverting the same back to fundamental mode have not been an easy task though lately there have been a number of promising studies reported on this technique [14, 15]. The virtual imaged phase array (VIPA) technique [11] utilizes convex or concave micromirrors to impart either negative or positive dispersion to a propagating pulse. However, dispersion compensation is achieved only at specific ITU grids though lately it has been shown that it can yield single-channel tunable dispersion compensation [16]. A myriad of other techniques for achieving dispersion compensation have been also proposed/demonstrated in the literature [7]. For example, one of the techniques involved electronically "prechirping" the signal pulses at the transmitter end [17–20]. Another technique involved compensation at the receiver end either using a heterodyne technique [21] or through nonlinear equalization in a direct-detection receiver [22]. Reference can be made to two additional optical techniques one involving Mach–Zehnder interferometer in a planar waveguide form [23], and the second, which involved midsystem spectral inversion (MSSI), in which dispersed signals in the first half of the link are phase conjugated at the midpoint of the span to invert the optical spectrum for reshaping the pulses [24]. Planar arrayed waveguides (AWG) have also been used as dispersion compensators [25, 26].

Out of all these, by far the DCF technique has been the most widely used technique [1]. One of the main advantages of this technical solution is that when appropriately designed it can provide a passive system, in principle, with negative chromatic dispersion coefficient D as high as -5000 ps/(nm·km) [27]. Such a scheme should compensate the positive chromatic dispersion over a relatively short length of the DCF and having low sensitivity to environmental influence (e.g., temperature, vibration, etc.) like that of the signal carrying fiber. Table 1 illustrates the comparative performance of various dispersion compensation techniques, which are potentially important.

In this particular review we focus on our extensive work on the basic DCF design originally proposed in [27, 28] and our subsequent realization of the same [29, 30]. Different variations in refractive index profiles have been simulated by us with several layers and different shapes, and a step index profile composed of two concentric spatially separated cores appears to give the best performances according to the fabrication constraints.

In the first part of this review we present the theoretical development and the simulation results on such a DCF and a study on the effect of an axial index dip (which often occurs in the MCVD process) on the optogeometrical tolerances of the designed fiber. This is followed by results and discussions on the actually fabricated DCF that we realized and which exhibits a very large negative D [$= -1800$ ps/(nm·km)] at wavelength 1.558 μm. This value of negative D to the best of our knowledge is the largest negative-dispersion DCF reported to date in the 1.55-μm

TABLE 1
Comparative Performance between Different Dispersion Compensation Techniques

Techniques	Performance	Main limitations
Prechirp technique	> −1000 ps/(nm·km) 150 km–5Gb/s	Electronic equipment
Nonlinear solutions	> −1000 ps/(nm·km) 5–6 Gb/s–80 km	Difficult for field deployment
Modal conversion	−700 ps/(nm·km)	Design of a two-mode DCF and modal converters for up and down conversion
Chirped FBC	−2000 ps/(nm·km)	Ripples in D vs λ, and requires temperature compensation
Interferometer	> −200 ps/(nm·km)	Over sensitivity to environments, e.g., vibration, temperature
VIPA	> −200 ps/(nm·km)	Automatic dispersion compensation for narrow passband
Dispersion compensating fiber	> −100 ps/(nm·km)	Refractive index profile design—Tolerances

window. The last part of the review is concerned with our study of the propagation behavior of this DCF in terms of connection, propagation, and bending losses as well as our most recent study to tailor these DCFs for broadband applications in DWDM transmission systems.

2. THEORETICAL DEVELOPMENT

The basic design of this DCF revolves around two spatially separated asymmetric concentric cores with a matched cladding. The refractive index profile is shown in Fig. 1. To model the propagation characteristics of this DCF, two numerical methods have been adopted: (i) matrix method [31], and (ii) a B.P.M. in cylindrical coordinates [32] in order to reduce the computation time. Due to symmetry in the refractive index profile, the B.P.M. technique requires only two coordinates (the radial and the axial ones) and use of the well-known slowly varying envelope approximation (SVEA) allows discretization of the radial and axial components of the field. By using the finite differences, the modes supported by the optical fiber were resolved by the WIJNANDS algorithm [33] that allows determination of the guided modes in the structure and the corresponding effective indices associated with them.

Several variations of the refractive index profile around the original basic design [27, 28] have been investigated, e.g., two or multicore segmented profiles, triangular profile, etc. with a targeted dispersion compensation at least 10 times better than the best reported in a DCF. For this purpose, the most effective one turned out to be a design, whose refractive index profile is shown in Fig. 1.

The composite index profile is similar to that of a directional coupler and hence supports two supermodes [27, 28]. These supermodes are characterized by a strong spatial redistribution of their modal fields as wavelength is varied. The parameters for the inner and outer cores were so chosen that the respective modes are phase

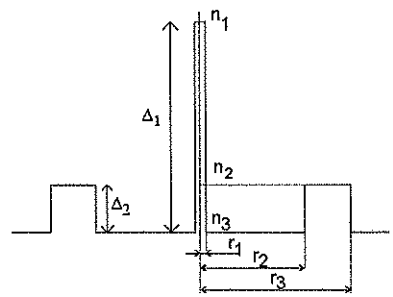

FIG. 1. Refractive index profile of the fiber (with $r_2/r_1 = 7.7$, $r_3/r_1 = 11$, $\Delta_1 = n_1 - n_3 = 0.0137$, $\Delta_2 = n_2 - n_3 = 0.0054$).

matched at a wavelength (λ_p) close to 1.55 μm. By investigating the wavelength-dependence of the fundamental supermode (see Fig. 2), it is seen that at wavelengths shorter than 1.55 μm the field is essentially confined to the inner core and for which the guide essentially functions like a step-index single-mode fiber, the effect of the outer core being negligible.

Around λ_p, optical coupling takes place between the inner and the outer core modes. At wavelengths longer than λ_p, however, most of the power of the fundamental mode spreads to the outer core and is effectively guided in the outer core. The fractional power in the second supermode of the fiber, which is orthogonal to the first supermode, is maximal in the outer core for wavelengths shorter than λ_p and it switches to the inner core for wavelengths longer than λ_p. This phenomenon induces a rapid change in the slope of the effective index (n_e) versus wavelength around 1.55 μm [27, 28]. Figure 3 depicts the variation of n_e as a function of the wavelength for the fundamental supermode.

The resulting chromatic dispersion coefficient of the fiber is then computed through the following formula:

$$D = \frac{-\lambda}{c}\frac{d^2 n_e}{d\lambda^2}. \tag{1}$$

A sample result corresponding to the fiber parameters in Fig. 1 is shown in Fig. 4. Since such a profile is easily attainable with common perform fabrication systems, e.g., the MCVD process, the minimum chromatic dispersion value can be better than -1000 ps/(nm·km) at the 1.55-μm-wavelength window through fine tuning of index profile parameters.

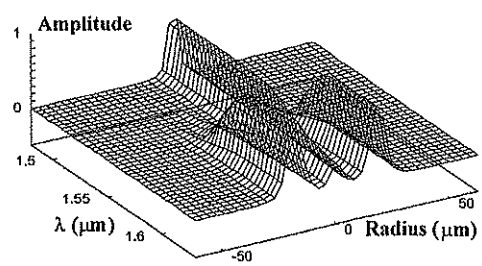

FIG. 2. Evolution of the modal amplitude of the fundamental supermode versus wavelength.

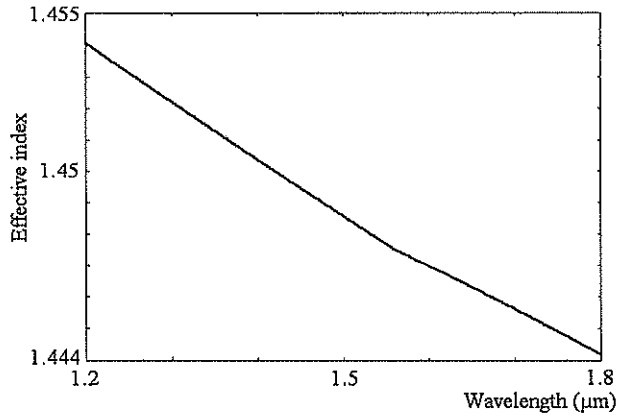

FIG. 3. Evolution of effective index of the fundamental supermode with wavelength.

For these calculations, we assume excitation of only the fundamental supermode of the fiber, which yields a high negative chromatic dispersion in the fiber. As mentioned above, the second supermode is also a natural mode of the structure, which yields a large positive chromatic dispersion. In view of this, in principle, it appears that it would perhaps be necessary to make a selective excitation of the DCF; a tapered fiber could be a possible solution [27, 28]. However, fortuitously in practice the second supermode appears to suffer a high transmission loss with propagation and virtually becomes extinct within a short length of the DCF.

3. TOLERANCES ON THE OPTOGEOMETRICAL PARAMETERS

In order to make an estimate of the tolerances involved in fabrication, we have computed the change of the dispersion characteristics of the DCF by introducing a 5% variation in the optogeometrical parameters of the fiber, which represents the maximum tolerances fixed by our MCVD fabrication process. A 5% variation in the radius of the inner core can lead to a shift of ~100 nm in the minimum dispersion wavelength and a variation in the chromatic dispersion value of up to 20% (Fig. 5).

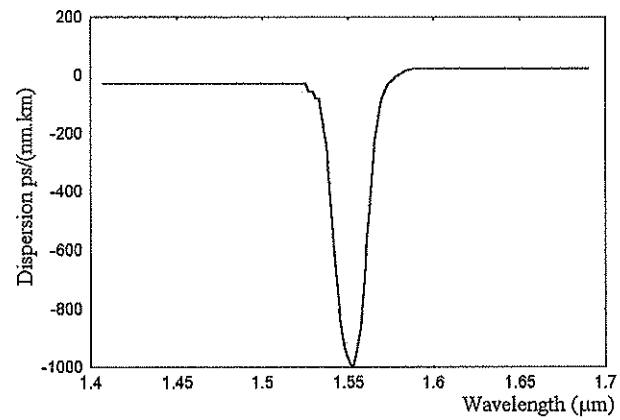

FIG. 4. Theoretical evolution of the chromatic dispersion versus wavelength.

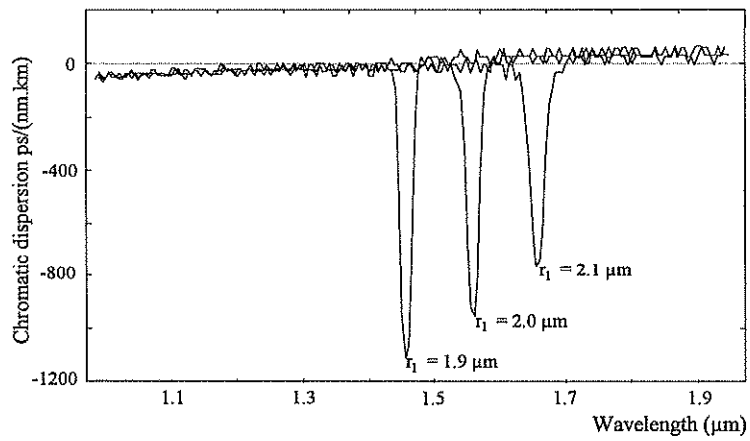

FIG. 5. Evolution of the chromatic dispersion with wavelength for different inner core radii.

A 5% variation in the value of the peak refractive index of the inner core can also lead to a shift of 100 nm of the minimum dispersion wavelength; the corresponding variations in profile parameters of the outer core lead to a shift of 50 nm of the minimum chromatic dispersion value. Thus these simulation results indicate that fabrication tolerances in the inner core are more stringent in order to ensure performance of the DCF close to the designed value.

Further it is known that an axial refractive index dip often occurs in MCVD fibers and unless properly controlled during the perform fabrication it may affect transmission characteristics of the fiber, e.g., location of the minimum dispersion wavelength [34]. In highly germania-doped fibers, the axial dip appears more prominently and we have thus studied the effect of such index profile imperfections on the performance of the DCF [35]. For this purpose, the assumed refractive index profile of the fiber with a central index dip is shown in Fig. 6 along with definition of a set of index profile parameters for which the calculations have been performed. The shape of the central index dip was assumed to be rectangular, triangular, or gaussian; a typical result for D vs λ with and without the dip is depicted in Fig. 7. To model the extent of the dip we introduce a parameter p as being equal to $n_1 - n_4$, n_4 as representing the minimum value of the refractive index across the index profile of the

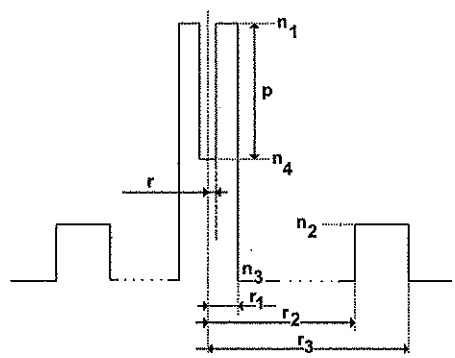

FIG. 6. Assumed refractive index profile of the fiber with central index dip.

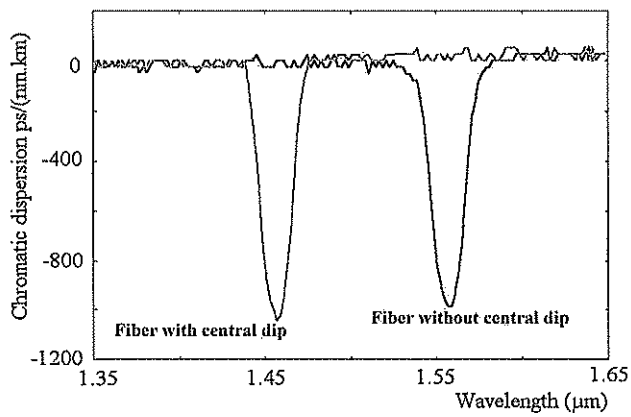

FIG. 7. Evolution of the chromatic dispersion with wavelength for a DCF with and without the central dip.

dip. It can be seen from Fig. 7 that the presence of the axial index dip induces a shift of the entire dispersion curve to shorter wavelengths; this is consistent with earlier studies on the same phenomenon reported on conventional single-mode fibers [34]. The small difference in magnitude of the peak negative dispersion value could be attributed to the fact that in the presence of the axial dip, the mode effective index and hence the modal field changes. Figure 8 shows evolution of λ_p in the DCF as a function of squared radius of the central dip for different depths of the dip as the labelling parameter.

It can be seen from Fig. 8 that the value of λ_p can undergo a shift by some hundreds of nanometers; for these calculations the radius of the inner core is assumed to be maintained all along at 2 μm. This curve also shows that if the radius of the central index dip doubles, the magnitude of the wavelength shift is four times larger than that of the case of "no-dip." In order to make a comparison between different geometries (e.g., rectangular, triangular) of the axial index dip, we have defined an equivalent area in terms of the product of the dip parameter p and the diameter $2r$ of the dip. It may be noted that this equivalent or effective core area

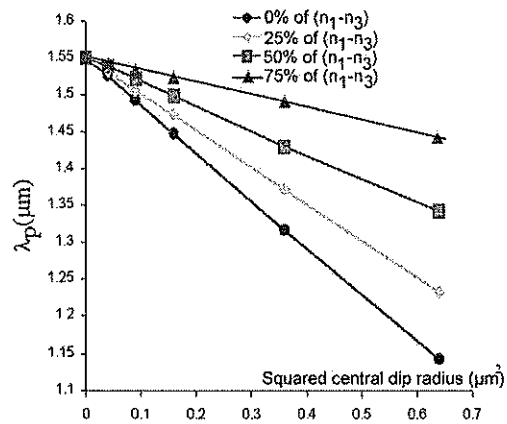

FIG. 8. Evolution of λ_p with squared radius for different central index dip depths.

is not related to the one usually defined to estimate nonlinear effects in single-mode optical fibers [37]. The above relation has been found to be very useful in the designing of practical DCFs with relatively larger inner core radii in order to realize the same propagation characteristics as that of a DCF without the central index dip. This important parameter has to be taken into account during the simulation stage to determine with precision the required outside cladding diameter of the DCF.

4. CHROMATIC DISPERSION IN DCF: EXPERIMENTAL RESULTS

The preform used in our experiment is made by the classical MCVD process. The chromatic dispersion of this DCF, several hundred meters, was measured by the phase-shift method [38], without trying to establish any particular launch condition (e.g., the taper or selective excitation system suggested in [27, 28]. These measurements were cross-checked many times and in many configurations.

The refractive index profile and the optogeometrical parameters of the realized fiber are given in Fig. 9.

The optimization of the MCVD process for the realization of the dual concentric core fiber leads to the design and realization of a fiber where the asymmetry of the two cores is very important in obtaining a large negative chromatic dispersion value. The fabricated fiber has a radius half that of the earlier simulated profile with a corresponding increase in Δ_1 by a factor of 2. The effect of some ripples in the real index profile of the preform are taken into account to determine precisely the outside diameter of the fiber.

Curve A, Fig. 10, represents the theoretical chromatic dispersion obtained through a 2-D BPM simulation from the real refractive index profile measured on the fiber. The measured dispersion is shown as curve B. It can be seen that the agreement between the simulation and the experimental results is very good; the value of the minimum chromatic dispersion is evaluated to be approximately -1800 ps/(nm·km) at 1.558 μm with a full width at half maximum (FWHM) of about 20 nm.

In order to establish the dispersion compensation by the fabricated DCF, we spliced about 30 m of this DCF with 4 km of a standard fiber (SMF28 optimized for 1.31 μm) and measured the chromatic dispersion of the link.

It is evident from Fig. 11 that the accumulated positive dispersion at the end of 4 km of SMF-28 fiber could be completely compensated for by the addition of only

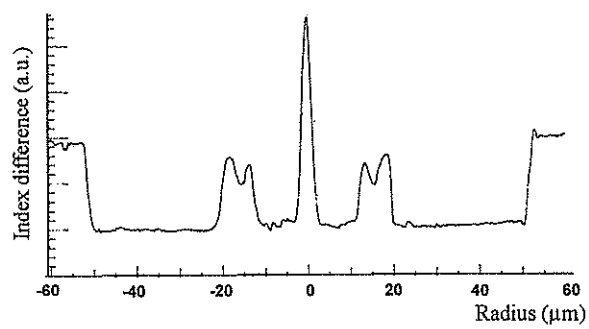

FIG. 9. Refractive index profile of the realized fiber (with $r_2/r_1 = 9.2$, $r_3/r_1 = 15.1$, $\Delta_1 = n_1 - n_3 = 0.03$, $\Delta_2 = n_2 - n_3 = 0.007$).

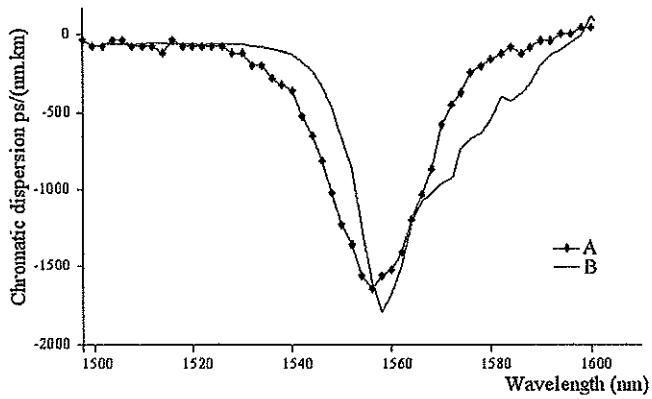

FIG. 10. Comparison between simulated (A) and measured chromatic dispersion (B) spectra.

a few tens of meters of the DCF and the spectral dependence of the link dispersion is as expected. The DCF inserted in to the link realizes the dispersion compensating function used without any particular injection conditions.

5. PROPAGATION IN THE DCF

As mentioned previously, no particular selective injection has been used and in order to examine the behavior of the DCF, we have investigated the energy distribution across the fiber cross section by launching light at the wavelengths of 0.633, 1.3, and 1.55 μm for different lengths of the DCF (1 m, 10 m, 300 m). Figure 12 depicts the typical observed energy distributions at the fiber output for different radial positions of light injection.

Table 2 summarizes the various observations made at the end of the fiber. The significant results are the following: at a wavelength lower than λ_p (1.55 μm in our application) it is possible to launch energy preferentially into the inner or the outer

FIG. 11. Evolution of the chromatic dispersion in a link composed of 4 km of a SMF28 fiber spliced with about 30 m of the fabricated DCF.

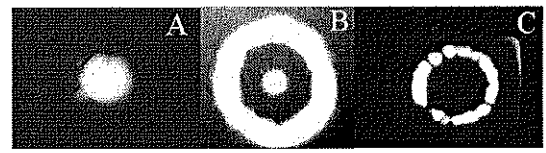

FIG. 12. Sample photographs of the fiber output end showing distribution of energy between the two cores at different wavelengths: (A) light in the central core only at 633 nm, (B) light distributed over the two cores as the supermode at 1550 nm, (C) light in the external core only at 633 nm.

core. At a wavelength close to λ_p, beyond a certain length of the fiber, the only possible distribution of energy is the one given by Fig. 12B. This distribution of energy represents the fundamental supermode of the structure [27, 28, 30]. Thus, as expected, in this fiber the spatial distribution of its supermode rapidly changes with wavelength. This behavior differs from what some authors attributed to a somewhat similar structure, namely coaxial fibers, which works like a directional coupler [39]. This difference can be attributed to the fact that the two cores which compose the fiber are highly asymmetric and relatively far away from each other.

A precise measurement of the near-field energy distribution at the output of the fiber as a function of wavelength shows a variation identical to the one depicted in Fig. 2, without any particular selective excitation. This shows that the second supermode is not guided in the fiber, due to the diffused light (leaky modes) observed exciting the outer core, we make the assumption that the surrounding core exhibits strong attenuation.

By introducing losses in the outer core, the simulations give the same results, only the fundamental supermode is guided. But in the process of the preform or fiber fabrication, no loss materials are introduced into the silica. So one explanation proposed is the coupling of the second supermode of the fiber to the leaky modes of the external core due in part to some noncircularity of the fiber cross section.

6. CONNECTION, PROPAGATION, AND BENDING LOSSES

Since the inner core radius of the DCF is smaller than that of the SMF-28 fiber, the insertion loss of the DCF is expected to be relatively large. Theoretical compu-

TABLE 2
Observed Distribution of Energy as a Function of Wavelength and Fiber Length

	633 nm	1300 nm	1550 nm
1 m	Internal, external	Internal, external	Internal, supermode, external
10 m	Internal, external	Internal, external	Internal, supermode, external (difficult)
300 m	Internal, external	Internal, external (difficult)	Internal (difficult), supermode

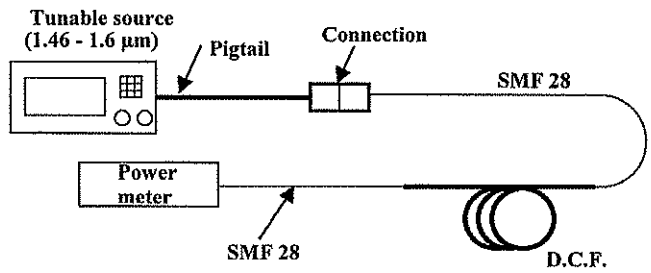

FIG. 13. Experimental setup for propagation and splice loss measurement.

tations show that due to the difference in mode field radii (MFR), the SMF–DCF connection loss is evaluated around 10 dB. Ideally, with tapered DCF ends, the overlap integral with the SMF can be sufficiently improved to reduce the connection loss to 1 dB.

By using multiple arc fusion splicing to connect the DCF to the SMF-28 fiber, the insertion losses could indeed be limited to 1.2 dB.

The experimental setup for the measurement of propagation and splice losses is given in Fig. 13. Two distinct measurements using the same experimental setup have been carried out. In the first case, the power exiting from the DCF (Fig. 14a) is directly measured; in the second case, the end of the DCF is spliced to a short length of SMF28, and the power is then measured at the end of the SMF28 (Fig. 14b). An initial measurement is carried out to eliminate the chromatic dependence of the several connections and to ensure that the experimental curves translate only the propagation losses of the DCF of length around 30 m.

Around λ_p the propagation losses are evaluated to be a few dB/km. Beyond λ_p the propagation losses increase substantially to some hundred of dB/km. The difference in attenuation between the two curves (Fig. 14b and Fig. 14a) around 1540 nm represents the connection loss of the last splice done with the SMF28 and is evaluated to be around 1.2 dB.

With the same set-up we have also determined the bending loss of a single loop of this DCF. The diameter of curvature varies between 0.2 and 4 cm. The variation of the bending loss with wavelength and for different curvature diameters is plotted in Fig. 15.

We can note that for small diameters and beyond λ_p, the bending loss increases rapidly for curvature diameters below 1 cm and for diameters more than 1 cm loss is limited to around 1 dB.

7. BROADBAND DISPERSION COMPENSATION

Rapid advancements in the technology of erbium-doped fiber amplifiers (EDFAs) and associated components have made possible high-capacity dense wavelength division multiplexed (DWDM) transmission spanning almost 80–90 nm of the EDFA gain spectrum. The demand for more and more bandwidth has led to a rapid increase in the channel count as well as in transmission at bit rates of 10 Gb/s or more per wavelength. In order to address the issue of broadband dispersion

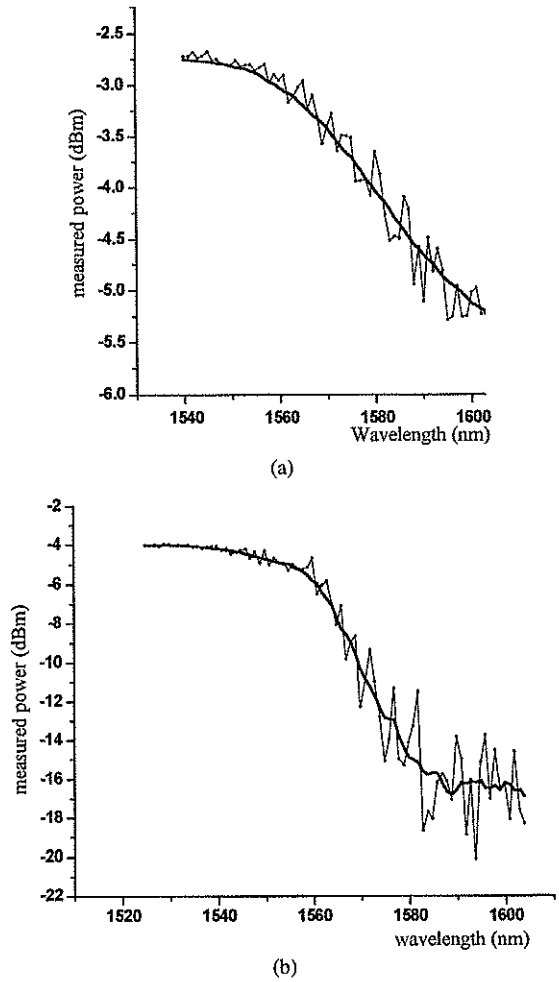

FIG. 14. Propagation losses in the DCF versus wavelength at the end of the DCF (a) and at the end of the SMF28 (b).

compensation in such DWDM links, we have recently carried out a profile tailoring exercise for such a DCF to make it suitable for achieving broadband compensation in the C-band (1530–1565 nm) as well as the L-bands (1570–1610 nm) of EDFAs [40, 41].

By a proper parameter optimization of the coaxial fiber structure, we can achieve dispersion values twice those of existing designs and it is possible to realize a dispersion-compensated link that is flattened (with the net dispersion being less than 1 ps/(nm·km)) over a wavelength range of 1.53 to 1.56 μm (see Fig. 16) [40].

We further optimized the profile parameters of the DCF in such a way that at 10 Gb/s, the residual dispersion of the combined DCF and conventional single mode fiber (CSF) is within the limit for a 1-dB chromatic dispersion penalty for a CSF link length of ~1000 km. The dispersion spectrum of the DCF and the dispersion spectrum of standard CSF are plotted in Figs. 17a and 17b for the C and L bands,

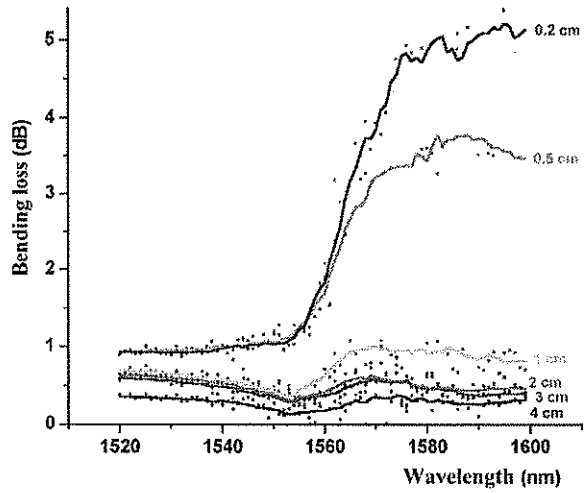

FIG. 15. Bending loss in the DCF versus wavelength for several bend diameters.

respectively. The parameters of the outer ring region were adjusted to maximize the effective area (A_{eff}) by tailoring the fiber parameters in order to obtain an $A_{\text{eff}} \sim 70\ \mu\text{m}^2$ at 1550 nm in the C-band and 1590 nm in the L-band, as compared to typical values of 20–25 μm^2 in conventional DCFs.

8. CONCLUSION

A dual concentric asymmetric core DCF has been designed and fabricated to achieve dispersion compensation at the 1.55-μm window. This fiber exhibits a negative chromatic dispersion coefficient $D = -1800$ ps/(nm·km) at 1.558 μm. To our knowledge this is the largest measured value in a DCF.

In this article we have studied the effect on the chromatic dispersion of the central dip obtained during the fabrication of the preform due to the M.C.V.D. process and evaluated the fabrication constraints of the designed fiber (optogeometrical

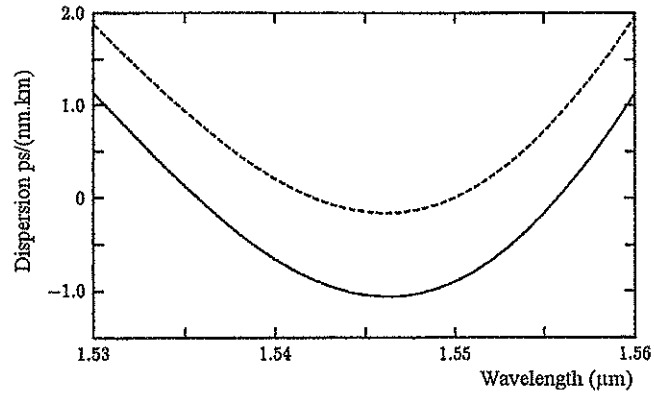

FIG. 16. Variation of dispersion of the total link consisting of 40 km of NDSF and 1.451 km (- - -) of DCF and that for a link consisting of 40 km NDSF and 1.525 km (—) of DCF for broadband dispersion compensation.

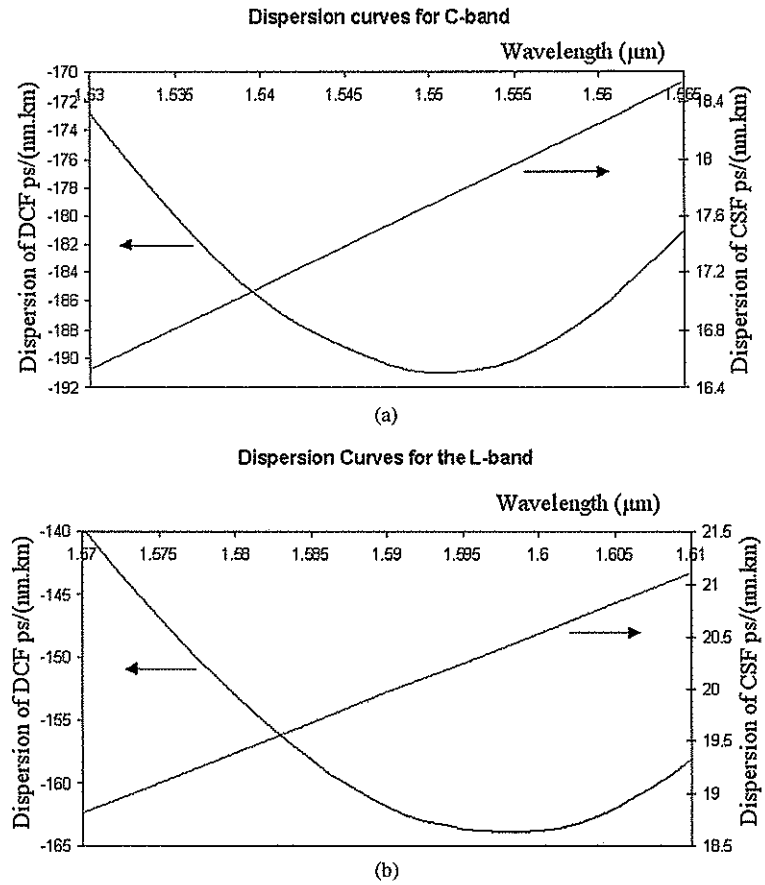

FIG. 17. Dispersion curves for DCF + CSF in the C band (a) and in the L band (b).

tolerances). We have shown that the induced shift may be important and can reach more than 100 nm.

We have also characterized the realized fiber in term of chromatic dispersion but also in term of propagation where we have studied the connection, bending and propagation losses.

ACKNOWLEDGMENTS

This work is supported by a collaborative project sponsored by the Indo French Center for the Promotion of Advanced Research (Centre Franco Indien pour la promotion de la recherche avancée), New Delhi. J.L.A. thanks the "Région Limousin" for its financial help; R.J. thanks the French Ministry of Education, Research and Technology (MNERT) for his fellowship.

REFERENCES

[1] V. Srikant, "Broadband dispersion and dispersion slope compensation in high bit rate and ultra long haul systems," in *Proc. OFC'2001*, papers TuH1-1 to TuH1-3, 2001.

[2] M. A. Saifi, S. J. Lang, L. G. Cohen, and J. Stone, "Triangular profile single mode fiber," *Opt. Lett.*, vol. 7, 43 (1982).

[3] G. P. Agrawal, *Nonlinear Fiber Optics*, Academic Press, San Diego, 1995.

[4] N. S. Bergano and C. R. Davidson, "Wavelength division multiplexing in long haul transmission systems," *J. Lightwave Technol.*, vol. 14, 1299 (1996).

[5] A. J. Lucero, S. Tsuda, V. L. da Silva, and D. L. Butler, "320 Gbit/s WDM transmission over 450 km of LEAF optical fiber," in *Proc. OFC/IOOC*, vol. 3, p. 215, 1999.

[6] A. K. Srivastava, Y. Sun, J. L. Zyskind, J. W. Sulhoff, C. Wolf, J. B. Judkins, J. Zhou, M. Zirngibl, R. P. Espindola, A. M. Vengsarkar, Y. P. Li, and A. R. Chraplyvy, "Error free transmission of 64 WDM 10 Gb/s channels over 520 km of Truewave fiber," in *Proc. ECOC*, vol. 1, 265, 1998.

[7] B. Jopson and A. Gnauck, "Dispersion compensation for optical fiber systems," *IEEE Commun. Mag.*, 96 (June 1995).

[8] D. Garthe *et al.*, "Adjustable dispersion equaliser for 10 and 20 Gbit/s over distances up to 160 km," *Electron. Lett.*, vol. 30, 2159 (1994).

[9] B. J. Eggleton *et al.*, "Recompression of pulses broadened by transmission through 10 km of nondispersion shifted fiber at 1.55 μm using 40 mm long optical fiber Bragg gratings with tuneable chirp and central wavelength," *IEEE Photon. Technol. Lett.*, vol. 7, no. 5, 494 (1995).

[10] C. D. Poole, J. M. Weisenfeld, and D. J. Giovanni, "Elliptical-core dual-mode fiber dispersion compensator," *Photon. Technol. Lett.*, vol. 5, 194 (1993).

[11] G. Ishikawa and H. Ooi, "Demonstration of automatic dispersion equalization in 40 Gbps OTDM transmission," in *Proc. ECOC'98*, Paper WdC06, p. 519 (1998).

[12] B. P. Pal, "All-fiber components," in *Electromagnetic Fields in Unconventional Structures and Materials*, A. Lakhtakia and O. N. Singh, Eds., Wiley, New York, 2000.

[13] M. Das and K. Thyagarajan, "Dispersion compensation in transmision using uniform long period fiber gratings," *Opt. Commun.*, vol. 190, 159 (2001).

[14] S. Ramachandran *et al.*, "All fiber, grating based, higher order mode dispersion compensator for broadband compensation and 1000 km transmission at 40 Gbs," in *Proc. ECOC'2000*, Paper PD-2.5, 2000.

[15] A. H. Gnauck, L. D. Garret, Y. Danziger, U. Levy, and M. Shur, "Dispersion and dispersion slope compensation of NZ-DSF for 40 Gbps operation over the entire C band," in *Proc. OFC 2000*, Paper PD-8, 2000.

[16] M. Shirasaki *et al.*, "Variable dispersion compensator using the virtually imaged phase array (VIPA) for 40 Gbps WDM transmission systems," in *Proc. ECOC'2000*, Paper PD2.3, 2000.

[17] B. Wedding, B. Franz, and B. Juginger, "10 Gb/s optical transmission up to 253 km via standard single mode fiber using the method of dispersion-supported transmission," *J. Lightwave Technol.*, vol. 12, 1720 (1994).

[18] B. F. Jørgensen, "Unrepeatered transmission at 10 Gbit/s over 204 km standard fiber," in *ECOC'94 Technical Digest*, Firenze, p. 685, 1994.

[19] G. May, A. Solheim, and J. Conradi, "Extended 10 Gb/s fiber transmission distance at 1538 nm using a duobinary receiver," *IEEE Photon. Technol. Lett.*, vol. 6, 648 (1994).

[20] A. J. Price and N. Le Mercier, "Reduced bandwidth optical digital intensity modulation with improved chromatic dispersion tolerance," *Electron. Lett.*, vol. 31, 58 (1995).

[21] N. Takachio, S. Norimatsu, and K. Iwashita, "Optical PSK synchronous heterodyne detection transmission experiment using fiber chromatic dispersion equalization," *IEEE Photon. Technol. Lett.*, vol. 4, 278 (1992).

[22] H. Winters and R. D. Gitlin, "Electrical signal processing techniques in long haul fiber optic systems," *IEEE Trans. Commun.*, vol. 38, 1439 (1990).

[23] K. Takiguchi, K. Okamoto, and K. Moriwaki, "Dispersion compensation using a planar ligthwave circuit optical equalizer," *IEEE Photon. Technol. Lett.*, vol. 6, 561 (1994).

[24] A. H. Gnauck *et al.*, "Transmission of two wavelength multiplexed 10 Gb/s channels over 560 km of dispersive fibre," *Electron. Lett.*, vol. 30, 727 (1994).

[25] H. Tsuda, K. Okamoto, T. Ishi, K. Nagnuma, Y. Inoue, H. Takenouchi, and T. Kusukowa, "Second and third order dispersion compensator using a high resolution arrayed waveguide grating," *IEEE Photon. Technol. Lett.*, vol. 11, 569 (1999).

[26] H. Tsuda, H. Takenouchi, A. Hirano, T. Kurokawa, and K. Okamoto, "Performance analysis of a dispersion compensator using arrayed waveguide gratings," *J. Lightwave Technol.*, vol. 18, 1139 (2000).

[27] K. Thyagarajan, R. K. Varshney, P. Palai, A. K. Ghatak, and I. C. Goyal, "A novel design of a dispersion compensating fiber," *IEEE Photon. Technol. Lett.*, vol. 8, no. 11, 1510 (1996).

[28] P. Palai, "Studies on dispersion compensating fibers and erbium doped fiber amplifiers," Ph.D. Thesis, Indian Institute of Technology, Delhi, 1997.

[29] J. L. Auguste, R. Jindal, J. M. Blondy, M. Clapeau, J. Marcou, B. Dussardier, G. Monnom, D. Ostrowsky, B. P. Pal, K. Thyagarajan "−1800 ps/(nm·km) chromatic dispersion at 1.55 μm in a dual concentric core fibre," *Electron. Lett.*, vol. 36, no. 20, 1689 (2000).

[30] J. L. Auguste, "Conception, réalisation et caractérisation d'une fibre à forte dispersion chromatique négative," *Thèse n° 12-2001*, Limoges, mars 2001.

[31] M. R. Shenoy, K. Thyagarajan, and A. K. Ghatak, "Numerical analysis of optical fibers using matrix approach," *J. Lightwave Technol.*, vol. 6, no. 8, 1285 (1988).

[32] J. Marcou, J. L. Augustè, and J. M. Blondy, "Cylindrical 2D beam propagation method for optical structures maintaining a revolution symmetry," *Opt. Fiber Technol.*, vol. 5, no. 1, 105 (1999).

[33] F. Wijnands, H. J. W. M. Hoekstra, J. M. Krijnen, and R. M. de Ridder, "Modal fields calculation using the finite difference beam propagation method," *J. Lightwave Technol.*, vol. 12, no. 12, 2006 (1994).

[34] B. P. Pal, A. Kumar, and A. K. Ghatak, "Effect of axial refractive-index dip on zero total dispersion wavelength in single-mode fibres," *Electron. Lett.*, vol. 16, no. 13, 505 (1980).

[35] J. L. Auguste, J. M. Blondy, M. Clapeau, J. Marcou, B. Dussardier, G. Monnom, and R. Jindal, "Design of a high negative chromatic dispersion in a single mode optical fiber: Effect of the central index dip," *Opt. Commun.*, vol. 178, 71 (2000).

[36] J. Marcou, Universite de Limoges, unpublished work.

[37] Y. Namihara, "Relationship between non-linear effective area and mode field diameter for dispersion shifted fibers," *Electron. Lett.*, vol. 30, no. 3, 262 (1994).

[38] Ref. ITU-T G650.

[39] A. C. Boucouvalas, "Coaxial optical fiber coupling," *J. Lightwave Technol.*, vol. 3, 1151 (1985).

[40] P. Palai, R. K. Varshney, and K. Thyagarajan, "A dispersion flattening dispersion compensating fiber design for broadband dispersion compensation," *Fiber Integrated Opt.*, vol. 20, 21 (2001).

[41] K. Pande and B. P. Pal, "Large effective area dispersion compensating fiber for broadband DWDM transmision," *submitted for publication* (2001).